Indonesian Journal of Fundamental and Applied Chemistry

Article http://ijfac.unsri.ac.id

Preparation of Palm Kernel Shell Binchotan for Radio Frequency Energy Harvesting

Nyimas Febrika Syabaniah^{1,3}, Nirwan Syarif^{2,3*}, Dedi Rohendi^{2,3}, Addy Rachmat^{2,3}, Rio Aldo Syahputra²

- ¹ Chemistry Program, Faculty of Computer and Natural Science, Universitas Indo Global Mandiri, Palembang, South Sumatera, 30129, Indonesia
- ² Chemistry Department, Faculty of Mathematic and Natural Sciences, Universitas Sriwijaya, Indralaya, Ogan Ilir, South Sumatera, Indonesia, 30662.
- ³ Center of Research Excellent in Fuel Cell and Hydrogen, Universitas Sriwijaya, Palembang, South Sumatera, Indonesia, 30128

Abstract

Research on the development of radio frequency energy harvesting slabs from palm kernel shells binchotan has been done. The slabs' were characterized by using XRD and FTIR instrumentation to determine their crystallography and functional groups. The electrical response of slabs was measured on impedance spectroscopy instrumentation. The conductivity, impedance, and dielectric constant were calculated from impedance spectroscopy data. Diffractograms showed peaks at 2θ , 24.5° and 44.56° , indicating the presence of crystalline carbon. FTIR analysis showed that carbon palm shells have absorption bands were observed in the range of $1100 - 1200 \text{ cm}^{-1}$ for CO of carboxylic acid, aldehyde, ketone, and ester, from $1475 \text{ to } 1600 \text{ cm}^{-1}$ for C=C aromatic ring and double peaks in $1900 - 2100 \text{ cm}^{-1}$ for conjugated C-C. The slab's conductivity varies from 1 to 7 mScm⁻¹. Impedance values for the slabs vary from 1.5 to 2.4 ohms. Dielectric constants for the slabs range from 0.42 to 140.

Keywords: impedance, dielectric, conductivity, acrylic, melamine, binchotan

Article Info

Received 3 September 2025
Received in revised 11
October 2025
Accepted 12 October 2025
Available Online 29
October 2025

Abstrak (Indonesian)

Penelitian tentang pengembangan kepingan penangkap energi frekuensi radio dari cangkang kelapa sawit binchotan telah dilakukan. Kepingan dikarakterisasi dengan menggunakan instrumen XRD dan FTIR untuk menentukan kristalografi dan gugus fungsinya. Respon listrik dari kepingan diukur dengan instrumentasi spektroskopi impedansi. Konduktivitas, impedansi dan konstanta dielektrik dihitung dari data yang spekstroskopi impedansi. Difraktogram menunjukkan puncak pada 2θ, 24.5° dan 44.56° yang menunjukkan adanya karbon kristalin. Analisis FTIR menunjukkan bahwa karbon cangkang kelapa sawit memiliki pita serapan yang dapat diamati pada kisaran 1100 – 1200 cm⁻¹ untuk Co dari asam karboksilat, aldehid, keton dan ester, dari 1475 – 1600 cm⁻¹ untuk cincin aromatik C=C dan puncak ganda pada 1900 – 2100 cm⁻¹ untuk C=C terkonjugasi. Konduktivitas kepingan bervariasi dari 1 hingga 7 mS/cm. Nilai impedansi untuk kepingan bervariasi daari 1,5 hingga 2,4 ohm. Konstanta dielektrik untuk kepingan berkisar 0,42 hingga 140.

Kata Kunci: impedansi, dielektrik, konduktivitas, akrilik, melamin, binchotan

INTRODUCTION

Energy harvesting, also known as energy scavenging, is the technique of obtaining energy from the environment [1]. For small, wireless autonomous devices, such as those found in wearable electronics and wireless sensor networks, energy harvesting is

generally defined as the process of obtaining energy from external sources, such as solar power, thermal energy, wind energy, salinity gradients, and kinetic energy, also referred to as ambient energy, and capturing and storing it. For low-energy electronics, energy harvesters supply relatively little power [2].

^{*}Corresponding Author: <u>nsyarif@unsri.ac.id</u>

The energy source for energy harvesters is ambient background, however the input fuel for some large-scale generation requires resources. For instance, there are temperature gradients caused by combustion engine activity and in cities; radio and television transmission contribute significantly to the environment's electromagnetic energy [3].

Radio frequency energy harvesting is feasible since the crystal radio was one of the first devices to ambient power gathered from electromagnetic radiation [4]. In the frequency range of about 20 kHz to about 300 GHz, radio frequency (RF) is the oscillation rate of an alternating electric current or voltage, or of a magnetic, electric, or electromagnetic field or mechanical system [5]. Peak detector, voltage elevator, matching circuit, and receiving antenna make up the fundamental components of a radio frequency energy harvesting system. The antenna picks up electromagnetic waves, the matching circuit amplifies the voltage, the peak detector converts the signal into a voltage value, and the voltage elevator adjusts the voltage output [6]. An effective antenna with a circuit that can convert alternating current (AC) voltage to direct current voltage is required for the RF energy harvesting technology [7]. One essential element for the RFEH system's successful operation is the front end. Its job is to record electromagnetic waves so that the integrated system can be powered later. The two resistances that make up the antenna impedance are the material resistance (Rloss) and the electromagnetic wave radiation resistance (Rs). Furthermore, the antenna structure affects impedance, which is typically capacitive for patch antennas and inductive for loop antennas. Thus, the primary component of an effective antenna is the material.

Ferrite is used as an antenna for magnetic field wireless power transfer by Radha *et.al.*[8]. It was verified that the suggested antenna could transmit a 5W magnetic field wireless power. In order to achieve wireless energy transmission with an optimal performance of -2.129 dB at 9.7 MHz operating frequency, Oruganti et al. used commercially available carbon fiber as a component of the transmitter and receiver antenna; the distance between the transmitter and receiver was 3 millimeters [9].

This paper reports composite materials from conductive carbon, i.e. binchotan and the binders, melamine and acrylic, for the antenna application. The mixtures were cast into slaps. Morphologic, crystallographic, and spectroscopic analyses were performed to describe their relationship with the performances. Their electrical responses were

evaluated by using impedance spectroscopy and calculated their properties. Therefore, this study aims to develop and characterize composite slabs from palm kernel shell binchotan and evaluate their electrical properties (conductivity, impedance, dielectric constant) to assess their potential as efficient and sustainable materials for RF energy harvesting antennas.

MATERIALS AND METHODS

Carbon Preparation

Palm shells were first cleaned using water and then cut into small pieces with a diameter of ± 1.5 cm, after the palm shell is cut into small pieces then the palm shell was sorted after the sorting process was carried out and the palm shell was filtered then the palm shell was dried under sunlight. 70 grams of dried palm oil shells were then put into a ceramic furnace. Palm shells in a ceramic furnace were then tightly closed and put into the heating wire oven to be heated to an initial temperature of 200 °C for 10 minutes. Every 10 minutes the temperature is raised 100 °C gradually until it reached 900 °C and hold for 1 hour. The ignited material was removed from the furnace with ceramic tongs and was immediately covered using wet sand to produce binchotan. The product was cleaned from dirt and washed with tap water. The cooled binchotan was then washed with water and dried. Disk mill-JIMO FF15 was employed to make binchotan powder.

Characterization of surface functional and carbon crystallography clusters

The characterizations of surface functional groups, morphology, and crystallography were carried out on palm kernel shell binchotan [10]. The functional groups contained in binchotan carbons were determined by the method, i.e. Fourier Transform InfraRed (FTIR). FTIR spectra obtained from measurement results carried out by Shimadzu Prestige 21 equipment run in DRIFT X-Ray Diffraction (XRD) patterns were produced from Shimadzu 7000 equipment using Cu $K\lambda$ radiation ($\lambda = 0.15406$).

Impedance spectroscopy analysis

Palm kernel shell binchotan powder produced from a disk mill was used to prepare monolithic microwave absorbent panels by mixing 30% w/w palm kernel shell binchotan powder with 70% acrylic resin as a binder. Slabs with a surface dimension of 450 x 450 mm² with a thickness of 3-75 mm were prepared. The mixture was stirred until homogeneous. A homogeneous mixture was poured evenly into a wooden mold while being swept slowly with a spatula

until polymerization occurred. The polymerization worked perfectly if the monolithic panel hardened. The hardened panel was removed from the mold and placed on a stainless sheet until the reflectivity measurements are made, and by comparison, a microwave absorbent monolithic panel was made using imported carbon, which was activated carbon (Sigma-Aldrich), and monolithic without using melamine resin, which was carbon that has not been made into powder. The adhesive was allowed to dry a little and glued while gently pressing on the surface of the slabs and held using a hydraulic pump. The same procedure was also applied for the comparison to palm kernel shell binchotan powder and 70/30 melamine.

Electrical responses were measured by the impedance method [11], that can be done using an oscilloscope, namely by measuring the AC mains voltage and the response voltage after crossing the reference resistance, R_e. A function generator was used to generate sine waves in the frequency range, 100 kHz to 900 kHz. The function generator was set to produce sine wave signals in both oscilloscope channels. A Channel 1 oscilloscope was used to measure the applied voltage, V1, while channel 2 was used to measure the voltage response by the sample, V2. V1 can be varied using impedance and conductivity.

The copper plate, which has been coated with palm kernel shell binchotan powder or commercial activated carbon as done in the previous process, was connected to a multimeter to measure resistance. Then the resistivity (ρ) was measured by the following formula:

$$\rho = \frac{R. A}{d} \tag{1}$$

$$K = \frac{d}{R - A}$$
 (2)

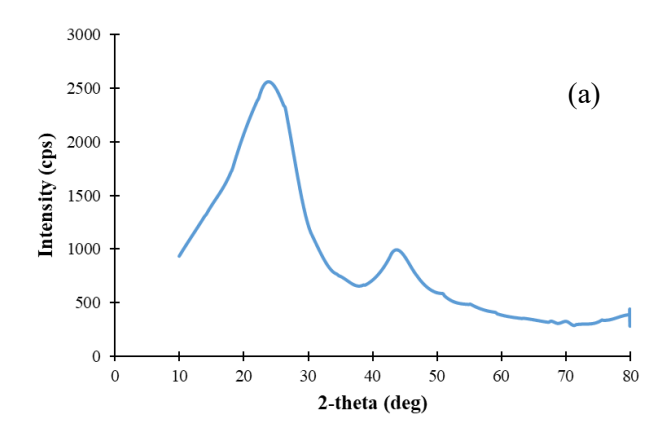
Where, R is resistance of palm kernel shell binchotan (ohm), d is distance of two probes, A is area under probe, and K is electrical conductivity. Whereas, the resistance of palm kernel shell binchotan powder or commercial activated carbon slabs were determined using a mathematical formula.

RESULTS AND DISCUSSION

Characterization XRD and FTIR of the Slabs

Diffractogram of palm kernel shell binchotan shows 2 peaks at $2\theta = 24.5^{\circ}$ and 44.26° which indicate the growth of crystals in the basal plane and the tip plane, in contrast with the commercial activated carbon. The absence of crystals in commercial activated carbon can be interpreted as amorphous. The diffraction peak pattern in **Figure** 1 (a) is evidence to the palm kernel shell binchotan that exhibits some

degree of crystalline according to their width and height. Similar results have been reported by wang *et all*. for the diffraction peaks of graphitic carbon nitride, at $2\theta = 25^{\circ}$ and $47^{\circ}[12]$. The orientation of the crystalline carbon is almost parallel. Inversely, the irregular pattern of the diffraction implies the carbon in amorphous form as reported by Kang *et al.* [13]. Similar results were reported by Nugraheni *et al.* and Manoj *et al.* where the diffractogram for carbon showed the irregularities as shown in **Figure** 1(b).



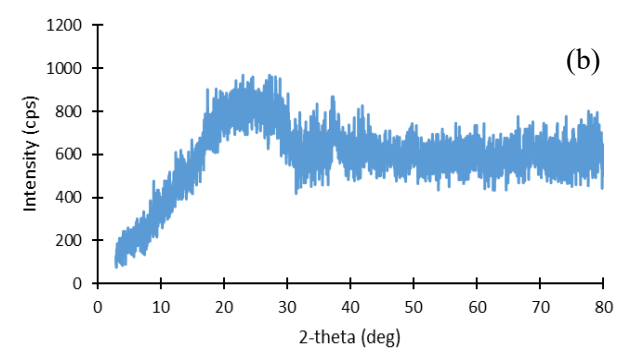


Figure 1. Diffractograms of (a) of palm kernel shell binchotan and (b) commercial activated carbon

FT-IR spectrum the palm kernel shell, binchotan and commercial activated carbon are seen in **Figure** 2. It is clear that palm kernel shell binchotan has a difference compared to commercially activated carbon based on a spectrogram. The peaks with wavelength ranges in the sample emerge with a strong wavelength range in the region of 2100-2260 cm⁻¹ indicating the existence of C=C functional groups. Whereas in commercial activated carbon there is no wavelength range which states that there is no C=C functional group. The FTIR spectrum of commercial activated carbon has 2 peaks that are not owned by the sample appear in the wavelength range $1600-1700 \text{ cm}^{-1}$ (C = O functional group) and wavelength range $3000-3700 \text{ cm}^{-1}$ (OH carboxylic acid functional groups).

However, in palm kernel shell binchotan a new peak appears that is not owned by commercial activated carbon, namely the wavelength range of 2100-2260 cm⁻¹ which indicates the presence of the C≡C functional group.

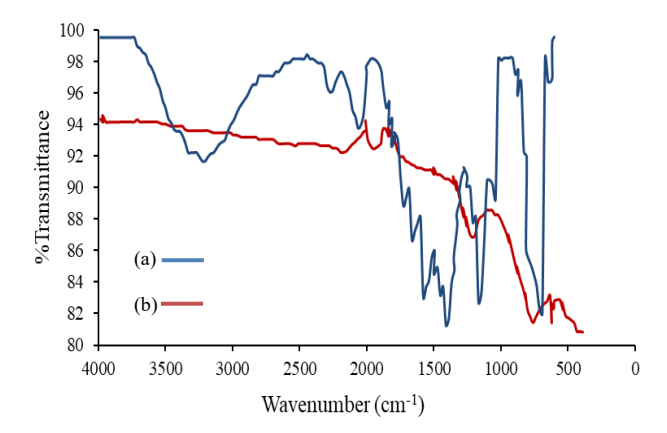


Figure 2. FTIR spectrum for (a) palm kernel shell binchotan and (b) commercial activated carbon.

Electrical conductivity measurement of the slabs

Electrical conductive material is a material that can conduct electricity [14]. The value of electrical conductivity is the opposite of the resistivity obtained from the resistance value of the slabs of palm kernel shell binchotan or commercial activated carbon mixed with melamine resin or acrylic resin to produce slabs. Resistance is the ability of a material to block the flow of electricity in ohms. The smaller the resistance value, the value of electrical conductivity of material will be greater. The value of the electrical conductivity of the slabs can be seen in **Figure** 3.

The results show that the highest conductivity, in low frequency was obtained from 30% palm kernel shell binchotan and 70% melamine, 7 mScm⁻¹. While the lowest value was obtained by mixing 30% commercial activated carbon and 70% melamine, 4.7 mScm⁻¹. Conversely, the mixture 30% palm kernel shell binchotan and 70% acrylic exhibited highest conductivity of 4.9 mScm⁻¹ in high frequency. The lowest conductivity value in highest frequency was obtained from 70% commercial activated carbon and 30% melamine < 1 mScm⁻¹. It can be seen that the use of less carbon can produce more conductive slabs. These results indicate that slabs use palm kernel shell binchotan fulfilled the requirement that the minimum carbon conductivity produced from pyrolysis is 1 mScm⁻¹ [15].

The higher the crystalline carbon content will get the higher the electrical conductivity as from palm kernel shell Binchotan [16]. The electrical conductivity of carbon materials occurs because there are more conjugated double bonds [17]. These double bonds can be found in aromatic carbon networks, for example, seen in naphthalene, phenanthrene and anthracene. Where the electron cloud in the structure of the compound will deliver the charge to the large structure across it (above and below). So that free electrons move in all directions, moving electrons in all directions produces electrical conductivity in carbon material. Therefore, it is potential to apply palm kernel shell binchotan in energy harvesting system. Such research has been done in the realization of radio frequency device antennas with carbon fiber composites.

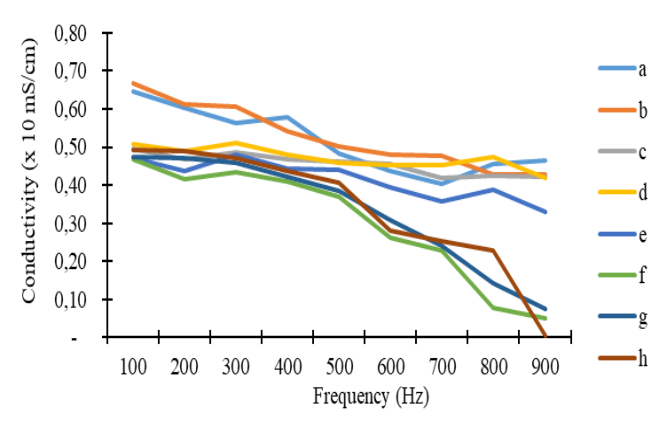


Figure 3. Impedance spectra of the slabs from: (a) 30% palm kernel shell binchotan + 70% acrylic, (b) 30% palm kernel shell binchotan + 70% Melamine, (c) 70% palm kernel shell binchotan + 30% acrylic, (d) 70% palm kernel shell binchotan + 30% Melamine, (e) 30% commercial activated carbon + acrylic 70%, (f) 30% commercial activated carbon + 70% melamine, (g) 70% commercial activated carbon + 30% acrylic, and (h). 70% commercial activated carbon + 30% melamine.

Impedances spectroscopy

The results of impedance spectroscopy analysis in **Figure** 4 show that the change in frequency greatly affects the impedance spectra of the slabs. The percentage of commercial activated and palm kernel shell binchotan content in the slabs give the opposite effect to each other. It can be seen that the slabs with palm kernel shell binchotan or commercial activated carbon has fluctuation in the impedance values with the tendency of decreasing as frequency increases. Impedance values for the slabs vary from 1.5 to 2.4 ohm.

It can be seen in **Figure** 4 that 70% commercial carbon or palm kernel shell binchotan content have the tendency to change impedance in reverse with 30% content. At low frequencies, the palm kernel shell binchotan gives the effect of decreasing the impedance. In contrast, the high content palm kernel shell binchotan causes an increasing in impedance as frequency is increased.

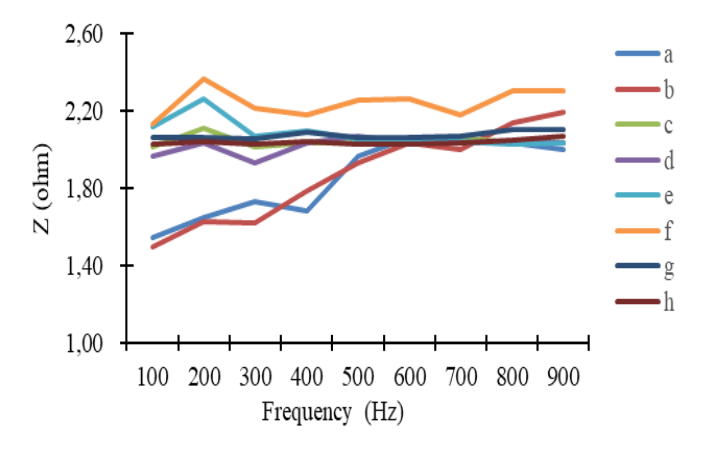


Figure 4. Impedance spectra of the slabs from: (a) 30% palm kernel shell binchotan + 70% acrylic, (b) 30% palm kernel shell binchotan + 70% Melamine, (c) 70% palm kernel shell binchotan + 30% acrylic, (d) 70% palm kernel shell binchotan + 30% Melamine, (e) 30% commercial activated carbon + acrylic 70%, (f) 30% commercial activated carbon + 70% melamine, (g) 70% commercial activated carbon + 30% acrylic, and (h). 70% commercial activated carbon + 30% melamine

The palm kernel shell binchotan relatively contains less functional groups compared to commercial activated carbon as shown in Figure 2. The existence of polar functional groups makes atoms and charged particles more easily oriented. The use of binder also causes electric orientation more easily in polar binder. The polar binder in this study is melamine binder [18]. This orientation causes the impedance value can be lower as shown in palm kernel shell binchotan slabs. While the acrylic binder is nonpolar that makes, the atoms in material are more difficult to orient [19]. The slabs impedance can be classified into two resistances: one is related to the material used (Rloss) and the other is due to the electromagnetic wave radiation (R_s) and the addition of the slabs structure. The slabs structure strongly depend on fabrication. Overall, if the slab has inductive character, then it is suitable for loop process.

Otherwise, if the slab has capacitive characters, then it is suitable for patch process.

Dielectric Constants

Important parameter for evaluating material for energy harvesting is dielectric constant. Dielectric properties are correlated with electro-optic properties of the crystals particularly when the materials were non-conducting [20]. Calculated dielectric constants for the slabs from impedance spectroscopy data can be shown in **Figure** 4.

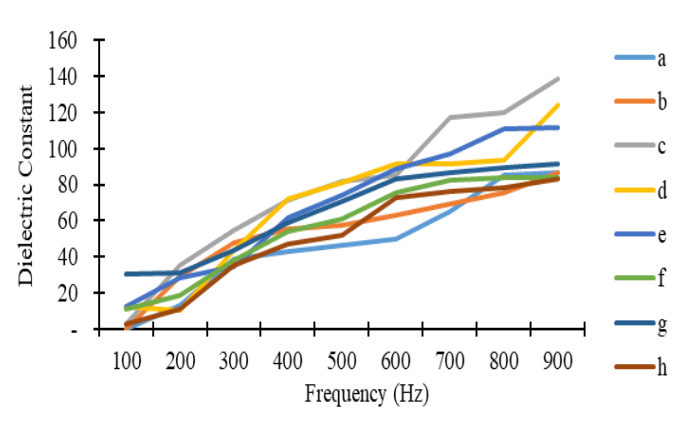


Figure 5. Dielectric constant of the slabs from: (a) 30% palm kernel shell binchotan + 70% acrylic, (b) 30% palm kernel shell binchotan + 70% Melamine, (c) 70% palm kernel shell binchotan + 30% acrylic, (d) 70% palm kernel shell binchotan + 30% acrylic, (d) 70% palm kernel shell binchotan + 30% Melamine, (e) 30% commercial activated carbon + acrylic 70%, (f) 30% commercial activated carbon + 70% melamine, (g) 70% commercial activated carbon + 30% acrylic, and (h). 70% commercial activated carbon + 30% melamine

Based on data on **Figure** 5, dielectric constants for the slabs range from 0.42 to 140. This value can be classified as high dielectric constant. High dielectric constant materials mainly contributed their capacitive properties. Pokorný *et all*. state that BaZr_xTi_{1-x}O₃ thin films and tailored polymer–ceramic composites exhibit dielectric constants in the range of 100–1400 while maintaining low dielectric loss, enabling efficient capacitive performance [21].

CONCLUSION

The slabs conductivity varies from 1 to 7 mScm⁻¹. Impedance values for the slabs vary from 1.5 to 2.4 ohm. Dielectric constants for the slabs range from 0.42 to 140. The slabs that content palm kernel shell binchotan can be employ as radiating patch. The slabs as antenna are having some advantages over conventional patch antenna like no metallic loss,

corrosion less, reduced skin effect, lower density, and high thermal conductivity. Microelectronic devices require new low dielectric constant materials as an interlayer dielectric. Carbons based slab are known as lightweight structures for the energy harvesting with conductive property. The reinforced polymers, i.e. epoxy or resin also affect the slabs conductivity. These results suggest the dependence impedance and dielectric constant on fabrication techniques and the frequency of the transmission. The slabs can be utilized as separator or receiver or antenna as they have low dielectric constant.

ACKNOWLEDGMENT

The author expresses gratitude and appreciation to Universitas Indo Global Mandiri for funding this research and to Universitas Sriwijaya through the Center of Research Excellence in Fuel Cell and Hydrogen, Universitas Sriwijaya.

REFERENCES

- [1] Huang X, Zhong T. Hydrokinetic Energy Harvesting from Flow-induced Vibration of a Hollow Cylinder Attached with a Bi-stable Energy Harvester. *Energy Conversion and Management*, 2023;278:116718.
- [2] Hasan MN, Sahlan S, Osman K, Mohamed Ali MS. Energy Harvesters for Wearable Electronics and Biomedical Devices. *Advanced Materials Technologies*, 2021;6(3):2000771.
- [3] Dolchinkov NT, Karaivanova-Dolchinkova BE. Impact of Types of Electromagnetic Radiation on Living Nature. In: *Environment Technologies Resources Proceedings of the International Scientific and Practical Conference*, 2023. p. 55–9.
- [4] Ibrahim HH, Singh MJ, Al-Bawri SS, Ibrahim SK, Islam MT, Alzamil A, et al. Radio Frequency Energy Harvesting Technologies: a Comprehensive Review on Designing, Methodologies, and Potential Applications. Sensors, 2022;22(11):4144.
- [5] Kokate PR. RF Energy Harvester. Sant Gadge Baba Amravati University, Amravati; 2023.
- [6] Mouapi A. Radiofrequency Energy Harvesting Systems for Internet of Things Applications: A Comprehensive Overview of Design Issues. *Sensors*, 2022;22(21):8088.
- [7] Bougas ID, Papadopoulou MS, Boursianis AD, Kokkinidis K, Goudos SK. State-of-the-art Techniques in RF Energy Harvesting Circuits. In: *Telecom*. MDPI; 2021. p. 369–89.
- [8] Radha SM, Choi SH, Lee JH, Oh JH, Cho I-K,

- Yoon I-J. Ferrite-Loaded Inverted Microstrip Line-Based Artificial Magnetic Conductor for the Magnetic Shielding Applications of a Wireless Power Transfer System. *Applied Sciences*, 2023;13(18):10523.
- [9] Arroyos V, Viitaniemi MLK, Keehn N, Oruganti V, Saunders W, Strauss K, et al. A Tale of Two Mice: Sustainable Electronics Design and Prototyping. In: *CHI Conference on Human Factors in Computing Systems Extended Abstracts*, 2022. p. 1–10.
- [10] Babatunde EO, Enomah S, Akwenuke OM, Ibeh MA, Okwelum CO, Mundu MM, et al. Preparation and Characterization of Palm Kernel Shell (PKS) Based Biocatalyst for the Transformation of Kernel Oil to Biodiesel. South African Journal of Chemical Engineering, 2025;52:200–10.
- [11] da Silva GMG, Faia PM, Mendes SR, Araujo ES. A Review of Impedance Spectroscopy Technique: Applications, Modelling, and Case Study of Relative Humidity Sensors Development. *Applied Sciences*, 2024;14(13):5754.
- [12] Wang L, Hong Y, Liu E, Wang Z, Chen J, Yang S, et al. Rapid polymerization synthesizing high-crystalline g-C3N4 towards boosting solar photocatalytic H2 generation. *International Journal of Hydrogen Energy*, [Internet]. 2020;45(11):6425–36. Available from: https://doi.org/10.1016/j.ijhydene.2019.12.168
- [13] Kang J, Yang X, Hu Q, Cai Z, Liu L-M, Guo L. Recent Progress of Amorphous Nanomaterials. *Chemical Reviews*, 2023;123(13):8859–941.
- [14] Gul' VE. Structure and Properties of Conducting Polymer Composites. CRC Press; 2023
- [15] Hadi ARA, Norazlina AS. The effects of pyrolysis temperature on chemical properties of empty fruit bunch and palm kernel shell biochars. *IOP Conference Series: Earth and Environmental Science*, 2021;757(1).
- [16] Jafri N, Yoon LW, Wong WY, Cheah KH. Power generation from palm kernel shell biochar in a direct carbon fuel cell. *SN Applied Sciences* [Internet], 2020;2(3):1–8. Available from: https://doi.org/10.1007/s42452-020-2189-2
- [17] Elnour AY, Alghyamah AA, Shaikh HM, Poulose AM, Al-Zahrani SM, Anis A, et al. Effect of pyrolysis temperature on biochar microstructural evolution, physicochemical characteristics, and its influence on

- biochar/polypropylene composites. *Applied Sciences*, 2019;9(6):7–9.
- [18] Jeong J, Jeon G, Ryu S, Lee JH. Ecofriendly and Electrically Conductive Cementitious Composites Using Melamine-Functionalized Biochar from Waste Coffee Beans. *Crystals*. 2022;12(6).
- [19] Chen B, Zhang Z, Xiao M, Wang S, Huang S, Han D, et al. Polymeric Binders Used in Lithium Ion Batteries: Actualities, Strategies and Trends. *ChemElectroChem*. 2024;11(14).
- [20] Bulathsinghala RL, Ravichandran A, Zhao H,

- Ding W, Dharmasena RDIG. The intrinsic impact of dielectric constant on output generation of triboelectric nanogenerators. *Nano Energy* [Internet], 2024;123(November 2023):109383. Available from: https://doi.org/10.1016/j.nanoen.2024.109383
- [21] Pokorný M, Klemeš J, Kotzianová A, Kohoutek T, Velebný V. Increased thickness uniformity of large-area nanofibrous layers by electrodynamic spinning. *AIP Advances* [Internet], 2017;7(10). Available from: http://dx.doi.org/10.1063/1.4998489